*34th EPS Conference on Plasma Phys. Warsaw, 2 - 6 July 2007 ECA Vol.**31F**, P-1.085 (2007)*

Coupled transport and turbulence simulations in the edge of tokamaks.

M. Vergote[1], M. Van Schoor[1], Y. Xu[1], R. Weynants[1], G. Van Oost[2]

[1] *Euratom-Etat Belge' - Associatie 'Euratom-Belgische Staat', Ecole Royale Militaire - Koninklijke Militaire School, Avenue de la Renaissance, Renaissancelaan 30, B-1000 Brussels, Belgium , Partner in the Trilateral Euregio Cluster (TEC).*

[2] *Department of Applied Physics, University of Gent, Rozier 44, 9000 Gent, Belgium*

1 Introduction

Turbulence, the major candidate to explain anomalous transport, can be quenched by sheared flows which rip the convective cells apart, thus forming a barrier. Electrostatic Reynolds stress (RS) on its own might be too small to explain the existence of the observed steady state sheared flow in the edge of a tokamak in the high-confinement regime. However, it can drive the so-called zonal flows(ZF), i.e. slowly fluctuating, radially sheared poloidal flows. In this paper we present coupled transport and turbulence simulations in the edge of the plasma. The turbulence is simulated locally on the basis of the Hasegawa-Wakatani(HW) equations, supplemented with background poloidal velocity terms. The background poloidal velocity and density profiles are evolved self-consistently by the corresponding transport equations, derived for momentum and particle density. For the particle transport, the procedure outlined in Ref. [1] has been adopted to couple the turbulence simulations to the transport code. Besides the particle transport, we compute the background poloidal velocity evolution self-consistently through the divergence of the Reynolds stresses that are produced on the different turbulence subdomains.

2 Setup of our model

One frequently applied method to retain profile modifications in the 2D Hasegawa-Wakatani model consists of assuming a separate evolution equation for the variational quantities [1]. We will extend this approach and apply it on a simplified rectangular slab of plasma. We thus subdivide the global turbulence problem in a number of independent subdomains (radially next to each other, at a distance $\sim 8\rho_S$ from each other, i.e. of the order of the radial correlation length; ρ_S is the drift scale length) and slowly varying variational quantities (determined by the 'transport' equation) between them. The radial position of each subdomain will be represented by X, in opposition to the inner coordinates (x,y) for grid points within each subdomain.

A radial gradient of the RS-component $\langle \underset{\sim}{v}_r \underset{\sim}{v}_\theta \rangle$ can drive a background poloidal velocity, similar to a radial divergence of the particle flux adapting the profile of the background density. The driving or damping forces due to both background profiles of density (n) and potential (ϕ) on the turbulence in the HW-system, can only be seen when we include background velocity terms in the standard HW model. Let us thus consider the set of extended HW equations, describing the turbulence in the presence of a background poloidal velocity $\vec{V}_b(x) = V_b \vec{u}_y = \partial_x \Phi_b'(x) \vec{u}_y$:

$$\left(\partial_t + (\vec{V}_b + \vec{v}_E)\cdot\vec{\nabla}\right)\nabla_\perp^2\phi'' = C_1(\phi'' - n'') + \frac{\partial^2 V_b}{\partial X^2}\frac{\partial\phi''}{\partial y} + C_2\nabla^2(\nabla_\perp^2\phi'')$$
$$\left(\partial_t + (\vec{V}_b + \vec{v}_E)\cdot\vec{\nabla}\right)n'' = C_1(\phi'' - n'') - \frac{\partial\phi''}{\partial y} + C_2\nabla^2 n'' \quad (1)$$

The doubly primed variables are expressed in the gyro-Bohm normalization [2]. Small symbols denote fast fluctuations, representing the high frequency turbulence on the independent subdomains. The capitals N and Φ denote background quantities, only depending on X and time t, while

$$N''(X,t) = \frac{L_N}{\rho_S}\frac{N(X,t) - N_b(X)}{N_b(X)} \qquad \text{and} \qquad \Phi''(X,t) = \frac{L_N}{\rho_S}\frac{e\Phi(X,t)}{k_B T_e} \quad (2)$$

are their normalized counterparts w.r.t. the reference normalizing values (variational quantities). The normalized fluctuating velocity $\vec{v}_E = (\frac{\vec{E}\times\vec{B}}{B^2})'' = (-\partial_y\phi'', \partial_x\phi'', 0)$ is determined by the stream function ϕ'', making the HW set nonlinear. The background quantities of the various fields are considered constant within the different subdomains. They can evolve only slightly from their reference values, so that the normalization does not change in time. Now $N_b(X)(1 + \frac{\rho_S}{L_N}N''(X,t))$ is the slowly in time varying background density, and $\Phi(X,t)$ the potential. Consistently, we have $C_1 \propto (N_b(1 + \frac{\rho_S}{L_N}N''))^{-1}$ evolving in time. The HW equations on the different subdomains, are implemented in an explicit manner in a pseudospectral code [3].

The transport equations under consideration, found by integrating Eqs. (1) over y and z (periodicity is assumed in the poloidal and toroidal direction), are written in physical units and provided with a source of particles at the inside-boundary of the domain to keep the turbulence sustained. The diffusive term (C_2) is neglected in the density equation. We solve the transport equations implicitly by a FEM technique ($\Gamma_N = \langle nv_{E,r}\rangle$ and written formally as $-D_{an}\partial_X N$ [1]):

$$\frac{\partial}{\partial t}N = -\vec{\nabla}\cdot\vec{\Gamma}_N + S_N, \qquad \text{or(impl.):} \qquad \frac{N^m - N^{m-1}}{\Delta t} = -\partial_X(-D_{an}^m\partial_X N^m) + S_N^m. \quad (3)$$

3 Anomalous particle transport determined by local turbulence simulations

When only this particle transport between the various subdomains is considered, the HW equations reduce to the original version ($V_b = 0$ in Eqs. (1)). The particle flux at different radii is determined by different independent local HW computations. The transport equation, Eq. (3), to which the particle flux Γ_N is the only time-dependent input, is solved at every turbulent HW time step (m). The resulting density profile –the driving force in the HW model– is updated and used in the next HW time step. Within a transport time step, the turbulence simulations can be regarded as iterations towards a converged state. In the saturated turbulence regime, a transport time step is then closed once the time-averaged particle flux satisfies a convergence criterion and does not change anymore in time: the density profile and the flux are then in agreement and we move on to the next transport time step. Because individual measurements of the anomalous particle flux have a noisy behavior, a smoothing ensemble average procedure is in place. We have 'validated' our procedure by running it on a model problem with a known analytical outcome (for $C_1 \geq 1$, see Ref. [2]). With respect to Ref. [1], our transport code is better suited to conserve particles as it is based on finite elements with cubic base functions.

Our aim is now to simulate aspects of the experimentally observed anomalous transport in the edge of TEXTOR. As normalization background density $N_b(X)$, we thus use a realistic density profile from the edge of TEXTOR. To keep this profile fixed in time, a source of particles is imposed at the inside of our X-domain (2 utmost inner HW subdomains in Fig. 1). The subdomains themselves are limited to $16\rho_S \times 16\rho_S$. An initial disturbance $N(X,t_0)$ is imposed, and the evolution from this starting density towards an 'equilibrium' is drawn in Fig. 1. The upper plots present the different indexed subdomains from inside ($r \approx 41$ cm, on the left) to the separatrix ($r \approx 46$ cm). The boundary conditions for the transport of the background density are of the Dirichlet type at the separatrix ($N|_{(X=X_{sep})} = 1\times10^{18}$), and of the Neumann type "zero-flux" at the inside ($\partial_X N|_{(X=X_{in})} = 0$). In case of Fig. 1, the radially integrated source represents $\sim 10^{19}$ m^{-2}s^{-1}, but it is apparently not sufficient to keep up the initial density profile.

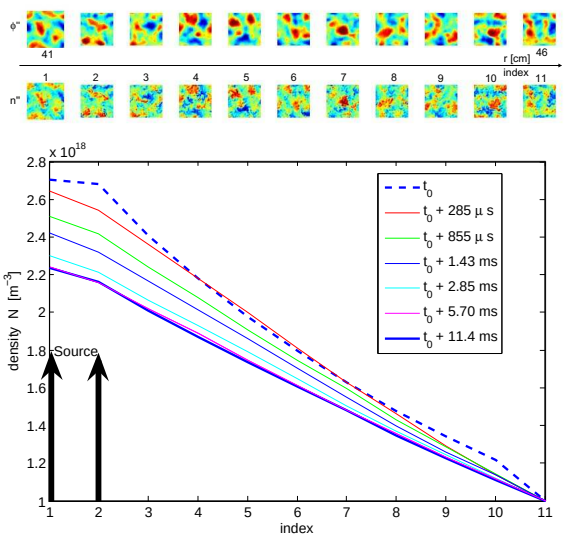

Figure 1: Snapshot of the 11 subdomains (upper =ϕ'' - lower row=n''). Bottom : Initial density profile being adapted towards an 'equilibrium' profile, for $t > 5$ ms.

4 Anomalous particle fluxes and Reynolds stress linking local turbulence simulations

Now we present the complete picture of the HW system for the fluctuations, Eq. (1), together with its two equations describing the variational quantities of N and Φ. We maintain the same procedure for the particle number transport as in the preceding section, with the same particle source in Eq. (3) and the same boundary conditions. But now, poloidal momentum is transferred as well between the different subdomains at every iteration within the transport time steps. This creation of a background vorticity profile, or equivalent poloidal velocity $V_b(X,t)$, is imposed in turn on the different subdomains at the subsequent time step.

The Reynolds stresses (anomalous momentum fluxes) determine the new vorticity profile,

$$\frac{\nabla_\perp^2 \Phi^m - \nabla_\perp^2 \Phi^{m-1}}{\Delta t} = -\frac{\partial}{\partial X}\left(\partial_X RS\right) + C_2 \frac{\partial^2}{\partial X^2}\left(\nabla_\perp^2 \Phi^m\right), \tag{4}$$

for which the same procedure of Eq. 3 can be used. After every turbulent iteration within a transport time step, the density $N(X,t_m)$ is updated as before and a new poloidal velocity profile is computed by numerically integrating the new vorticity profile. The imposed boundary conditions can be summarized as $V_b|_{(X=X_{sep})} = 0$ and $\frac{\partial}{\partial x} V_b|_{(X=X_{sep})} = 0$ at the separatrix and $\partial_X V_b|(X = X_{in}) = cst$ at the inside.

A simulation with ZF (allowed by putting $C_1 = 0$ for all $k_y = 0$-components in all subdomains [4]) and Reynolds stress transport between the subdomains switched on, starts from the same initial conditions as in Fig. 1. The initial velocity profile is completely flat.

In Fig. 2 we plot the background density $N(X,t)$ evolution at the different subdomains. This simulation is running until $t \approx 16$ms, with the same constant parallel wavenumber. The density increases, pointing to the formation of a natural transport barrier. It is only after 10 ms that a stationary background density profile is found. Compared to the evolution towards the equilibrium without ZF and Reynolds stress as plotted in Fig. 1, it takes more time for the nonlinear generation of ZF inside the subdomains to find an equilibrium with the momentum transport and the changing density $N(X,t)$. Furthermore, we see an oscillatory behavior of the poloidal velocity in time (not shown here), with increasing amplitudes towards the centre of the torus. In the innermost subdomains, poloidal velocities of the order of 100 m/s are found, i.e. reasonable values compared to the experimentally measured Geodesic Acoustic Modes ZF in TEXTOR [5].

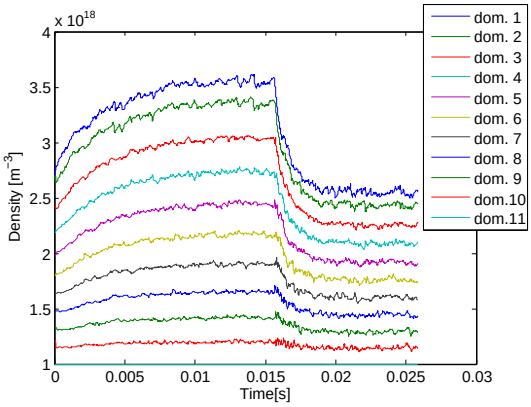

Figure 2: Background density *N* evolving in time (subdomains 1-11).

A subsequent simulation started from the stationary situation at $t \approx 16$ms, in Fig. 2. At this moment, the parallel coupling coefficient C_1 is lowered to 40 % of the preceding value (reduction of the electron's adiabaticity). In reality, this drop could be caused by an increase of the plasma's (parallel) resistivity or –eventually– by an increase of the parallel wavelength. We remark now a much faster response to this change, having a direct effect on the local transport levels. Not only the particle transport reacts faster, also the momentum transport shows an abrupt reaction, with temporarily higher rms-fluctuation levels.

5 Conclusion

With the simple HW model, we tried to simulate the coupling between transport and turbulence in the edge. In Sec. 3, only particle transport was taken into account between the independent local simulations. From a slightly too steep density profile, the background density slowly relaxes to a new 'equilibrium' profile. In Sec. 4, we switched on the momentum transport (RS fluxes) and allowed the creation of ZF (all other parameters are kept unchanged). The density profile steepens (instead of relaxing), showing that one kind of a transport barrier is formed.

References

[1] A.I. Shestakov. *J. Comput. Phys.*, 185:399, 2003.

[2] M. Vergote. PhD thesis, Univ. Gent, 2007.

[3] Karniadakis. *J. Comput. Phys.*, 97:414, 1991.

[4] B. Scott. In *Proceedings of the Joint Varenna-Lausanne Int'l Workshop*, p. 413, 2000.

[5] A. Kramer-Flecken et al. *Phys. Rev. Letters*, 97(4), 2006.